Identifying factors influencing corrosion rate in reinforced concrete under simulated natural climate

Aditi Chauhan[1,*] and Umesh Kumar Sharma[2]

[1]Department of Civil Engineering, Indian Institute of Technology Bombay, Mumbai 400 076, India
[2]Department of Civil Engineering, Indian Institute of Technology Roorkee, Roorkee 247 667, India

The influence of various parameters on corrosion rate in reinforced concrete was examined using analysis of variance for crack initiation and crack propagation phases. Water–cement (w/c) ratio was found to be the most significant factor before the onset of concrete surface crack, followed by the time of wetting. In the crack propagation phase, contribution of w/c ratio reduced while time of wetting and external chloride concentration became prominent. The concrete cover values of 30 mm and 60 mm affected the corrosion rate marginally. The diameter of reinforcing steel and spacing between bars were the least contributing factors to the corrosion rate under both phases.

Keywords: Chloride ions, corrosion rate, crack initiation and propagation, natural climatic conditions, reinforced concrete.

TIME to corrosion initiation, i.e. time for chloride ions to exceed the threshold limit on the rebar and break the passivating layer, has been adopted as the service life prediction criterion across the globe for a considerable amount of time[1–4]. However, the eventual shift in defining the service life by incorporating the propagation phase led to the development of many concrete damage models with predefined limit states of cover cracking, loss in steel cross-section, loss in stiffness, loss in structural carrying capacity, etc.[5–15]. All these models depend on a factor defined as corrosion rate (i_{corr}). It is clear from the literature that corrosion rate is a function of various parameters[16–24] and several studies have presented ways of quantifying i_{corr} of reinforcing steel in terms of these variables[25–30]. Many laboratory studies have been carried out under controlled temperature and relative humidity conditions to quantify the effect of these factors on corrosion propagation. Only a few account for the corrosion rate values in the real environment. Therefore, it becomes necessary to determine the effect of various parameters on i_{corr} in the natural environment and develop a model representative of actual i_{corr} in reinforced concrete (RC) structures. The present study helps identify the most influential parameters affecting corrosion rate in RC under laboratory-simulated natural climatic variations. The Taguchi method of design and analysis was used in the study to identify the factors contributing to the corrosion propagation period, which was further divided into two phases: crack initiation and crack propagation.

Experimental procedure

This section details the materials used, fabrication of test specimens and accelerated corrosion test procedure adopted to achieve the desired aim.

Materials

Ordinary Portland cement (OPC) in the Indian market was used to prepare all the concrete mixtures. This was combined with potable water, river sand and graded crushed granite with maximum grain size of 20 mm and 12.5 mm in the ratio 1.5 : 1.

Accelerated corrosion test

The prepared RC specimen with three TMT steel bars, i.e. two corners and one middle bar is shown in Figure 1. An

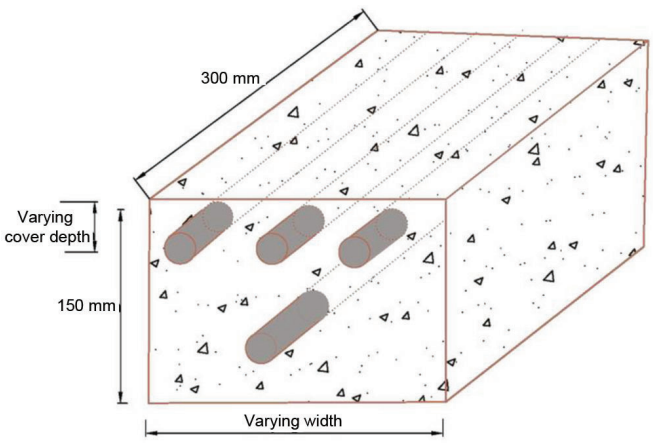

Figure 1. Reinforced concrete specimen subject to corrosion.

*For correspondence. (e-mail: chauhan.aditi1@gmail.com)

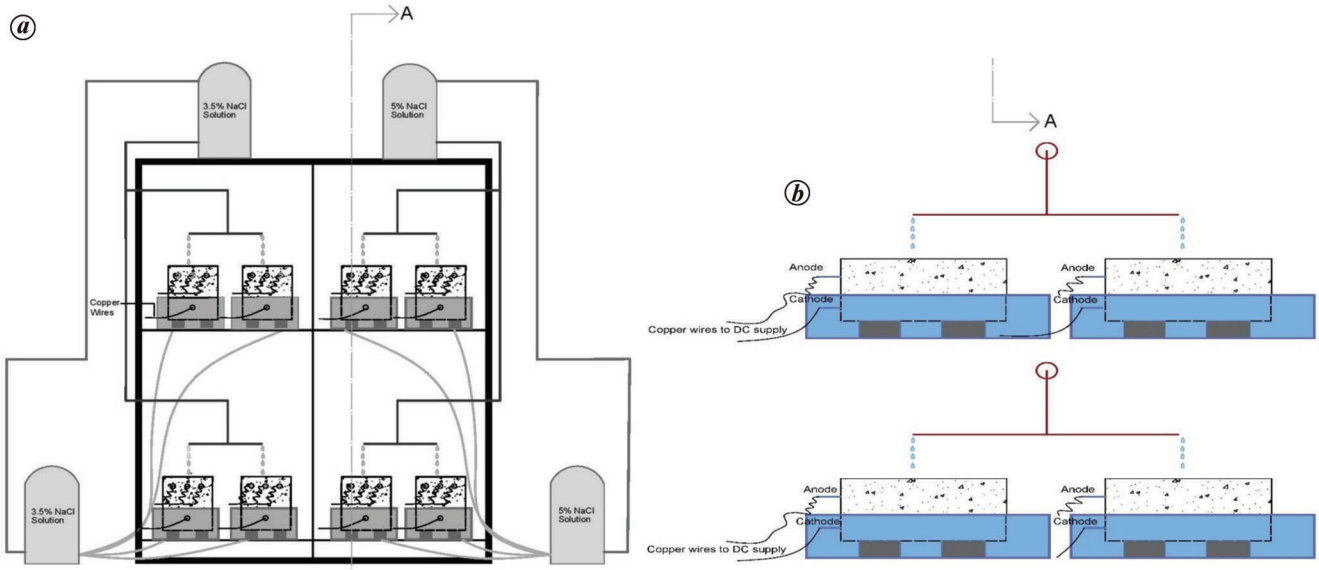

Figure 2. Schematic of experimental set-up to carry out Taguchi design of experiments. ***a***, Section showing corrosion set-up inside the environment chamber. ***b***, Section *A–A*.

Table 1. Factors and levels for Taguchi design and analysis

Factors	Level 1	Level 2
A: Time of wetting (TOW; days)	3	5
B: Chloride concentration (Concentration; %)	3.5	5
C: Water–cement ratio (w/c)	0.4	0.5
D: Concrete cover depth (Cover; mm)	30	60
E: Diameter of rebar (Diameter; mm)	8	12
F: Spacing between rebars (Spacing; mm)	48	63

accelerated corrosion test procedure was adopted to achieve the target crack width of 0.3 mm in the RC specimens under chloride-induced corrosion. A stainless steel rod of 10 mm diameter, which acted as the cathode in accelerated corrosion tests, was placed below the middle steel bar at a constant spacing in all the specimens. Alternate wet–dry cycles with externally supplied (impressed) voltage were used to accelerate the corrosion process in the test specimens.

To account for the effect of natural climate on the corrosion process, the testing was carried out in a laboratory environment chamber simulating daily variations in temperature and relative humidity for a typical Indian marine city. Similar climatic conditions are found in marine cities in the north of Australia, west of Brazil, southwest of Mexico and some centrally located African countries. Wet–dry cycles to simulate corrosion in the RC specimens were achieved by wetting them with a salt solution and then allowing them to dry in the chamber climatic conditions (Figure 2). Simultaneous application of an impressed constant voltage of 15 V during the wetting cycles was achieved using an external direct current (DC) supply. Once the wetting period for a specimen was completed in a weekly cycle, the drying period was maintained for the remaining duration. Figure 2 shows the schematic of the experimental set-up adopted in this study.

Corrosion rate for each specimen was determined, details of which are provided in the following sections.

Design of experiments (Taguchi design)

The present experimental study uses an orthogonal array as given by Taguchi to analyse the experimental design and determine the order in which various parameters influence corrosion rate.

Design parameters and levels: It is imperative to consider the effect of environmental factors along with the material and geometric properties of the structural elements while carrying out service-life studies of RC structures. Table 1 lists the parameters chosen at two different levels to carry out the analysis. The present case limits the number of levels for each parameter to two and can be increased to three or four levels depending on the availability of time and space.

As shown in Table 2, the Taguchi method of design was employed using the defined parameters and levels. Eight sets of experiments denoted by *E–X*, where *E* means experiment and *X* refers to the experiment number, i.e. from 1 to 8, were analysed for corrosion rate. Three identical specimens were tested for accelerated corrosion under each experiment.

Experimentation: Accelerated corrosion testing was conducted on the RC specimens in the environmental chamber, simulating temperature and relative humidity variations, as already explained in the previous section. To shorten the corrosion initiation phase, the specimens were initially subject to the electro-migration of chloride ions under 30 V, as given by Xia *et al.*[31].

Table 2. Taguchi design with results for corrosion rate

Experiment	Factors						Phase-1		Phase-2	
	A	B	C	D	E	F	i_{corr} (Average of corner bars; μA/cm^2)	i_{corr} (Middle bar; μA/cm^2)	i_{corr} (Average of corner bars; μA/cm^2)	i_{corr} (Middle bar; μA/cm^2)
E-1	3	5	0.4	30	8	43	0.69	0.99	0.75	0.91
E-2	3	5	0.4	60	12	68	0.57	0.59	0.59	0.58
E-3	3	3.5	0.5	30	8	68	1.46	1.57	0.68	0.94
E-4	3	3.5	0.5	60	12	43	0.80	1.00	0.56	0.51
E-5	5	5	0.5	30	12	43	1.50	2.13	0.85	1.52
E-6	5	5	0.5	60	8	68	1.61	1.47	1.85	2.07
E-7	5	3.5	0.4	30	12	68	0.96	0.80	0.69	0.56
E-8	5	3.5	0.4	60	8	43	0.96	0.97	0.64	0.67

Table 3. Taguchi analysis results for corner and middle bars showing ranking of parameters

Level	TOW	Concentration	w/c	Cover	Diameter	Spacing
Phase-1 (corner bar)						
1	0.880	1.045	0.798	1.154	1.180	0.988
2	1.258	1.094	1.341	0.984	0.959	1.151
Delta	0.377	0.049	0.544	0.17	0.222	0.163
Rank	2	6	1	4	3	5
Phase-2 (corner bar)						
1	0.644	0.641	0.666	0.741	0.977	0.698
2	1.007	1.010	0.985	0.910	0.674	0.953
Delta	0.363	0.370	0.318	0.169	0.304	0.256
Rank	2	1	3	6	4	5
Phase-1 (middle bar)						
1	1.035	1.082	0.835	1.371	1.248	1.271
2	1.342	1.295	1.542	1.006	1.129	1.106
Delta	0.307	0.212	0.707	0.364	0.118	0.165
Rank	3	4	1	2	6	5
Phase-2 (middle bar)						
1	0.736	0.672	0.679	0.982	1.146	0.902
2	1.204	1.269	1.261	0.958	0.794	1.038
Delta	0.468	0.597	0.582	0.025	0.352	0.136
Rank	3	1	2	6	4	5

w/c, Water–cement ratio.

The reference silver/silver chloride electrode was measured half cell potential (HCP) values on each specimen. The HCP values reached the threshold for corrosion activity, i.e. –250 mV for all specimens, almost after a week[32]. This was followed by accelerated corrosion tests under an impressed voltage of 15 V and wet–dry cycles to determine the corrosion rate for all three steel bars in each specimen using the galvanostatic pulse method (GPM)-based device at the end of every wet–dry cycle. In addition, concrete surface crack width values were also measured weekly using a crack measuring microscope with a least count of 0.05 mm.

Results and discussion

Analysis of Taguchi design

The Taguchi experimental design was analysed for corrosion rate in two different phases. As suggested by Otieno *et al.*[20], corrosion rate values were averaged up to the point when the crack width reached a value of 0.3 mm. Average values of corrosion rate were determined separately for the corner and middle bars under each phase and analysis of the experimental design was performed for these bars.

Table 2 shows the corrosion rate results for the developed sets of experiments under both phases. Using the average test values presented in Table 2, it is possible to determine the effect of individual parameters at different levels on corrosion rate. The mean corrosion rate for corner bars at a specified level was calculated and termed the level mean average. Here, the level mean average for parameter *A* at level 1 was found to be 0.88 under phase-1 using the average values of the means (0.69, 0.57, 1.46 and 0.80) taken from E-1, E-2, E-3 and E-4. Table 3 shows the level mean averages of each design parameter at different levels, indicating representative values of corrosion rate in the corner and middle bars for phase-1 and phase-2.

The difference between the maximum and minimum level mean average gave ranks, which indicated the order of the influence of the six design parameters on the corrosion rate

Table 4. ANOVA analysis results for corner and middle bars

Source	Sum of squares (SSK)	Mean square	*F*-value	Percentage contribution
Phase-1 (Corner bar)				
Factor A	0.285	0.285	12.75	25.60
Factor B	0.005	0.005	0.22	0.44
Factor C	0.591	0.591	26.47	53.15
Factor D	0.058	0.058	2.59	5.20
Factor E	0.098	0.098	4.4	8.83
Factor F	0.053	0.053	2.38	4.79
Error	0.022	0.022	–	–
Total (SST)	1.113	–	–	–
Phase-2 (Corner bar)				
Factor A	0.264	0.264	1.77	20.92
Factor B	0.273	0.273	1.83	21.66
Factor C	0.203	0.203	1.36	16.05
Factor D	0.057	0.057	0.38	4.55
Factor E	0.185	0.185	1.24	14.64
Factor F	0.131	0.131	0.87	10.34
Error	0.149	0.149	–	–
Total (SST)	1.262	–	–	–
Phase-1 (Middle bar)				
Factor A	0.189	0.189	1.49	10.77
Factor B	0.090	0.090	0.71	5.13
Factor C	1.000	1.000	7.88	57.02
Factor D	0.265	0.265	2.09	15.13
Factor E	0.028	0.028	0.22	1.59
Factor F	0.055	0.055	0.43	3.12
Error	0.127	0.127		–
Total (SST)	1.754			–
Phase-2 (Middle bar)				
Factor A	0.438	0.438	32.08	20.57
Factor B	0.713	0.713	52.25	33.50
Factor C	0.678	0.678	49.69	31.86
Factor D	0.001	0.001	0.09	0.06
Factor E	0.248	0.248	18.15	11.64
Factor F	0.037	0.037	2.70	1.73
Error	0.014	0.014	–	–
Total (SST)	2.129	–	–	–

SST, Total sum of squares.

in both phases (Table 3). It is clear from Table 3 that the ranking of the parameters changes when corrosion propagates from phase-1 to phase-2.

Analysis of variance

Once the ranks of all the parameters are determined for both phases, it is essential to quantitatively evaluate each parameter's contribution to the corrosion rate. This was accomplished by ANOVA to predict percentage contribution of each parameter on corrosion rate, which was determined using eq. (1) and is provided in Table 4 for the corner and middle bars under both phases.

$$\text{Percentage contribution of each parameter} = \frac{\text{SSK}}{\text{SST}} \times 100, \quad (1)$$

where SSK is sum of squares and SST is the total sum of squares.

ANOVA indicated that the percentage contribution of different parameters varied with the occurrence of cracks in the RC specimens.

Effect of time of wetting

It was observed that increasing the time of wetting increased the corrosion rate (Figure 3). An increase in the time of wetting exposed the specimen to the corroding environment for a longer duration. A previous study found an inverse relationship between the time of wetting and corrosion rate[33]. This is due to more oxygen being available during longer drying periods for cathodic reactions to occur, resulting in a greater corrosion rate. In the present study, the specimens were subjected to variations in climate during the drying period representative of a typical marine city of the

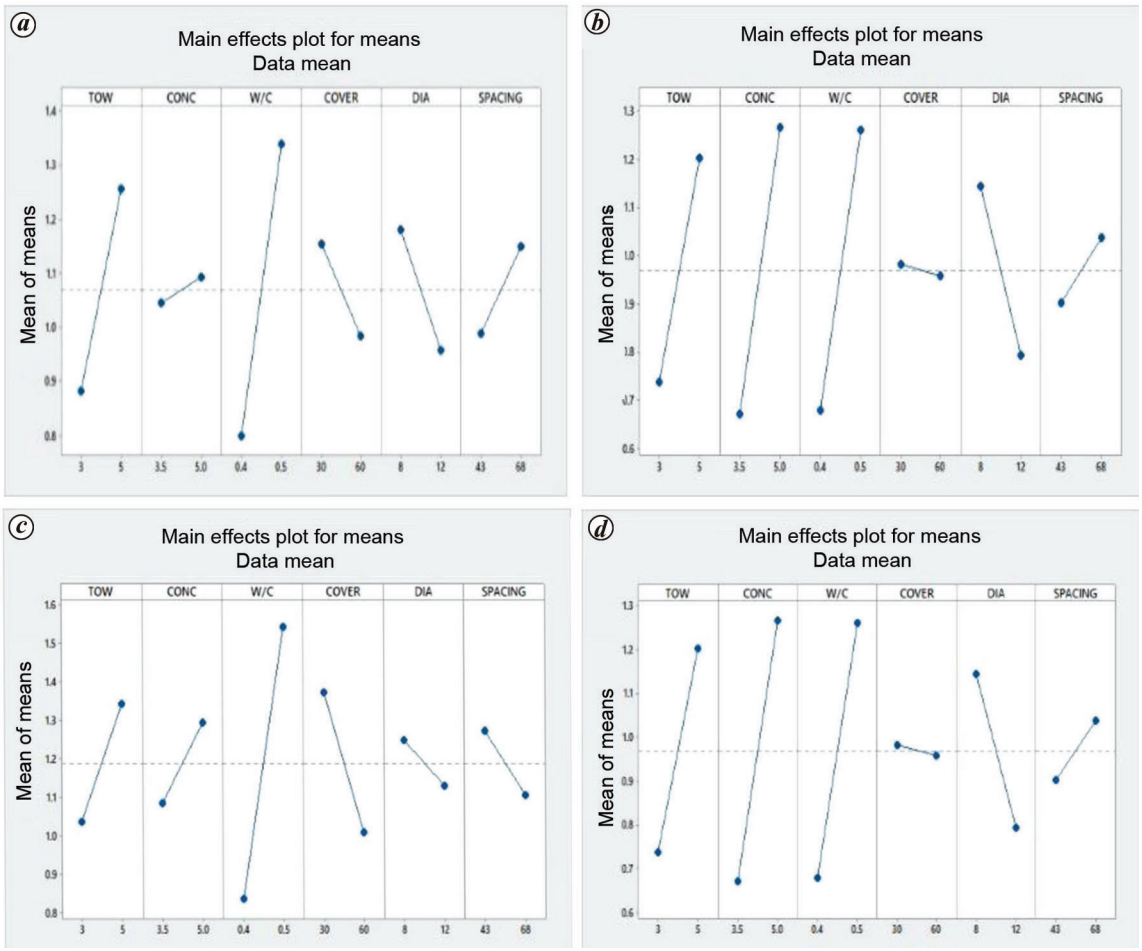

Figure 3. Effect of various parameters on corrosion rate before and after the appearance of surface cracks. ***a***, ***b***, Corner bar: (***a***) phase-1 and (***b***) phase-2. ***c***, ***d***, Middle bar: (***c***) phase-1 and (***d***) phase-2.

Indian subcontinent, which is characterized by high relative humidity. Concrete pores get blocked at high relative humidity, resulting in discontinuity of interconnected pores and, therefore, shortage of oxygen in such environments.

Effect of external chloride concentration

In the present study corrosion rate for uncracked concrete, i.e. during phase-1 remained unaffected by varying the external chloride concentration values between 3.5% and 5% (Table 4). However, during phase-2, the dependence of chloride concentration on the corrosion rate increased (Table 4). For the cracking phase, the reinforcing steel bars came in direct contact with the external environment, i.e. salt solution through cracks running from the concrete surface to the rebar surface. The electrochemical cell potential depends on the concentration of the electrolyte, allowing change in anodic and cathodic potential on the rebar surface and affecting corrosion rate. Increased salt concentration resulted in higher corrosion rates for both the corner and middle bars after cracking.

Effect of w/c ratio

A lower corrosion rate was observed at water–cement (w/c) ratio of 0.4 compared to that at w/c 0.5, which is evident from the slope of the line in Figure 3. The contribution of w/c ratio was found to be the highest among all the factors considered in this study during phase-1. During phase-2, the influence of w/c ratio reduced considerably (Table 4).

Effect of concrete cover depth

In the present study, for the adopted cover depth values of 30 and 60 mm, the reduction in i_{corr} was less with an increase in cover thickness. Concrete cover affects the corrosion rate mainly by governing the travel path of the corrosion agents (oxygen, moisture), but the present case suggests that this parameter has a lower effect than the w/c ratio. Similar observations were made by Balabanić *et al.*[19] for concrete cover thicknesses of 50 and 100 mm, along with w/c ratios of 0.4 and 0.7. The values chosen for cover depth in the present study and by Balabanić *et al.*[19] are higher than the minimum

required to cover in the design codes. Therefore, it would be appropriate to conclude that the corrosion rate is not much affected by concrete cover values greater than 30 mm.

Effect of rebar diameter

The present study shows a reduction in corrosion rate for a 12 mm reinforcing bar compared to an 8 mm bar. ANOVA showed a small contribution of rebar diameter to corrosion rate for both the corner and middle bars before and after cracking.

Effect of spacing between bars

The analysis showed that increased spacing slightly increased the corrosion rate (Figure 3). However, variations in response using the chosen spacing values were found insignificant compared to other variables in this study (Table 4).

Conclusion

The Taguchi design of experiments was employed to study the effect of various key parameters on corrosion rate in RC under laboratory-simulated natural climatic conditions. The rate of corrosion in two phases of corrosion propagation, i.e. before the onset of the surface crack and when the crack width reached a value of 0.3 mm, was analysed using the Taguchi analysis and ANOVA. The following conclusions can be drawn from the results.

(1) Water–cement ratio is the most significant factor influencing corrosion rate before the onset of surface crack and its contribution decreases with the appearance of concrete surface cracks.

(2) Time of wetting of RC structures also influences the corrosion rate before the initiation of cracking, i.e. larger the wetting time higher the corrosion rate. Even after the onset of cracking, this environmental parameter significantly affects the corrosion rate and therefore should be considered in the durability design.

(3) External chloride concentration, the diameter of reinforcing bar and spacing between the bars have been found to have a negligible effect on corrosion rate before surface cracking. However, with the onset of surface cracking, their influence on corrosion rate increases and chloride concentration is the most contributing factor amongst these three factors.

(4) Corrosion rate is not much affected by the range of concrete cover values (30 and 60 mm) or the spacing between the bars (43 and 68 mm) chosen in this study.

(5) High relative humidity in the environment results in a higher rate of corrosion for shorter drying periods. This trend is opposite to what has been observed in most previous studies, suggesting the importance of considering the natural climatic conditions while estimating corrosion rate.

1. de Medeiros-Junior, R. A., de Lima, M. G. and de Medeiros, M. H. F., Service life of concrete structures considering the effects of temperature and relative humidity on chloride transport. *Environ. Dev. Sustain.*, 2014, **17**, 1103–1119.
2. Liang, M. T., Wang, K. L. and Liang, C. H., Service life prediction of reinforced concrete structures. *Cem. Concr. Res.*, 1999, **29**, 1411–1418.
3. Bentz, E. C., Probabilistic modeling of service life for structures subjected to chlorides. *ACI Mater. J.*, 2003, **100**, 391–397.
4. Jiao, J. T., Ye, Y. H., Wang, C. F. and Ye, G. C., The reliability analysis of the initiation time for RC members under chlorine salt ingress and local micro-climate. *Mater. Sci. Forum*, 2016, **866**, 134–138.
5. Nossoni, G., Asce, A. M., Harichandran, R. S. and Asce, F., Electrochemical–mechanistic model for concrete cover cracking due to corrosion initiated by chloride diffusion. *J. Mater. Civ. Eng.*, 2014, **26**.
6. Cao, C., Cheung, M. M. S. and Chan, B. Y. B., Modelling of interaction between corrosion-induced concrete cover crack and steel corrosion rate. *Corros. Sci.*, 2013, **69**, 97–109.
7. Chen, E. and Leung, C. K. Y., A coupled diffusion–mechanical model with boundary element method to predict concrete cover cracking due to steel corrosion. *Corros. Sci.*, 2017, **126**, 180–196.
8. Zhao, Y., Dong, J., Wu, Y. and Jin, W., Corrosion-induced concrete cracking model considering corrosion product-filled paste at the concrete/steel interface. *Constr. Build. Mater.*, 2016, **116**, 273–280.
9. Ožbolt, J., Oršani, F. and Balabani, G., Modeling damage in concrete caused by corrosion of reinforcement: coupled 3D FE model. *Int. J. Fract.*, 2012, **178**, 233–244.
10. Michel, A., Geiker, M. R., Stang, H. and Lepech, M. D., Integrated modelling of corrosion-induced deterioration in reinforced concrete structures. In *EUROCORR*, Estoril, Spain, 2013, pp. 1–5.
11. Thybo, A. E. A., Michel, A. and Stang, H., Smeared crack modelling approach for corrosion-induced concrete damage. *Mater. Struct.*, 2017, **50**, 1–14.
12. Dagher, H. and Kulendran, S., Finite element modeling of corrosion damage in concrete structures. *ACI Struct. J.*, 1992, **89**, 699–708.
13. Guzman, S., Galvez, J. C. and Sancho, J. M., Modelling of corrosion-induced cover cracking in reinforced concrete by an embedded cohesive crack finite element. *Eng. Fract. Mech.*, 2012, **93**, 92–107.
14. Zhang, J., Ling, X. and Guan, Z., Finite element modeling of concrete cover crack propagation due to non-uniform corrosion of reinforcement. *Constr. Build. Mater.*, 2017, **132**, 487–499.
15. Jamali, A., Angst, U., Adey, B. and Elsener, B., Modeling of corrosion-induced concrete cover cracking: a critical analysis. *Constr. Build. Mater.*, 2013, **42**, 225–237.
16. Otieno, M., Beushausen, H. and Alexander, M., Prediction of corrosion rate in RC structures – a critical review. In *Modelling of Corroding Concrete Structures*, RILEM Book Series 5, 2011, pp. 15–37.
17. Scott, A. and Alexander, M. G., The influence of binder type, cracking and cover on corrosion rates of steel in chloride-contaminated concrete. *Mag. Concr. Res.*, 2007, **59**, 495–505.
18. Balabanić, G., Bićanić, N. and Dureković, A., Mathematical modeling of electrochemical steel corrosion in concrete. *J. Eng. Mech.*, 1996, **122**, 1113–1122.
19. Balabanić, G., Bićanić, N. and Dureković, A., The influence of w/c ratio, concrete cover thickness and degree of water saturation on the corrosion rate of reinforcing steel in concrete. *Cem. Concr. Res.*, 1996, **26**, 761–769.
20. Otieno, M. B., Alexander, M. G. and Beushausen, H.-D., Corrosion in cracked and uncracked concrete – influence of crack width, concrete quality and crack reopening. *Mag. Concr. Res.*, 2010, **62**, 393–404.
21. Isgor, O. B. and Ghods, P., The effect of temperature on the corrosion of steel in concrete. Part 1: simulated polarization resistance tests and model development. *Corros. Sci.*, 2009, **51**, 415–425.
22. Hervert, H. L. Z. and Mendez, R. C., Identifying factors influencing the corrosion rate of steel using nonparametric statistics. *Int. J. Electrochem. Sci.*, 2012, **7**, 6343–6352.

23. Villagrán Zaccardi, Y. A., Bértora, A. and Di Maio, Á. A., Temperature and humidity influences on the on-site active marine corrosion of reinforced concrete elements. *Mater. Struct.*, 2013, **46**, 1527–1535.
24. Otieno, M., Beushausen, H. and Alexander, M., Chloride-induced corrosion of steel in cracked concrete – Part I: experimental studies under accelerated and natural marine environments. *Cem. Concr. Res.*, 2016, **79**, 373–385.
25. Liu, Y. and Weyers, R. E., Modeling the time-to-corrosion cracking in chloride contaminated reinforced concrete structures. *ACI Mater. J.*, 1998, **95**, 675–681.
26. Raupach, M., Models for the propagation phase of reinforcement corrosion – an overview. *Mater. Corros.*, 2006, **57**, 605–613.
27. Mart, B., Service life modelling of reinforced concrete structures exposed to chlorides, Ph.D. thesis, University of Toronto, 1999.
28. Jung, W. Y., Yoon, Y. S. and Sohn, Y. M., Predicting the remaining service life of land concrete by steel corrosion. *Cem. Concr. Res.*, 2003, **33**, 663–677.
29. Vu, K. A. T. and Stewart, M. G., Structural reliability of concrete bridges including improved chloride-induced corrosion models. *Struct. Saf.*, 2000, **22**, 313–333.
30. Otieno, M., Beushausen, H. and Alexander, M., Chloride-induced corrosion of steel in cracked concrete – Part II: corrosion rate prediction models. *Cem. Concr. Res.*, 2016, **79**, 386–394.
31. Xia, J., Jin, W.-L. and Li, L.-Y., Effect of chloride-induced reinforcing steel corrosion on the flexural strength of reinforced concrete beams. *Mag. Concr. Res.*, 2012, **64**, 471–485.
32. John, H., Bungey, S. G. M. and M. G. G., *Testing of Concrete in Structures*, Taylor and Francis, Milton Park, Abingdon, England, 2006.
33. Golden, G., The effect of cyclic wetting and drying on the corrosion rate of steel in reinforced concrete. MS thesis, University of Cape Town, 2015.

Received 6 April 2021; accepted 28 August 2022

doi: 10.18520/cs/v123/i11/1327-1333